

---

# Low-Rank Graph Contrastive Learning for Node Classification

---

Yancheng Wang<sup>1</sup>

Yingzhen Yang<sup>1</sup>

<sup>1</sup>School of Computing and Augmented Intelligence, Arizona State University, Tempe, AZ 85281, USA, {ywan1053, yingzhen.yang}@asu.edu

## Abstract

Graph Neural Networks (GNNs) have been widely used to learn node representations and with outstanding performance on various tasks such as node classification. However, noise, which inevitably exists in real-world graph data, would considerably degrade the performance of GNNs revealed by recent studies. In this work, we propose a novel and robust GNN encoder, Low-Rank Graph Contrastive Learning (LR-GCL). Our method performs transductive node classification in two steps. First, a low-rank GCL encoder named LR-GCL is trained by prototypical contrastive learning with low-rank regularization. Next, using the features produced by LR-GCL, a linear transductive classification algorithm is used to classify the unlabeled nodes in the graph. Our LR-GCL is inspired by the low frequency property of the graph data and its labels, and it is also theoretically motivated by our sharp generalization bound for transductive learning. To the best of our knowledge, our theoretical result is among the first to theoretically demonstrate the advantage of low-rank learning in graph contrastive learning supported by strong empirical performance. Extensive experiments on public benchmarks demonstrate the superior performance of LR-GCL and the robustness of the learned node representations. The code of LR-GCL is available at [https://anonymous.4open.science/r/Low-Rank\\_Graph\\_Contrastive\\_Learning-64A6/](https://anonymous.4open.science/r/Low-Rank_Graph_Contrastive_Learning-64A6/).

Welling, 2017, Bruna et al., 2014, Hamilton et al., 2017, Xu et al., 2019]. Most prevailing GNNs [Kipf and Welling, 2017, Zhu and Koniusz, 2020] leverage the graph structure and obtain the representation of nodes in a graph by utilizing the features of their connected nodes. Benefiting from such propagation mechanism, node representations obtained by GNN encoders have demonstrated superior performance on various downstream tasks such as semi-supervised node classification and node clustering.

Although GNNs have achieved great success in node representation learning, many existing GNN approaches do not consider the noise in the input graph. In fact, noise inherently exists in the graph data for many real-world applications. Such noise may be present in node attributes or node labels, which forms two types of noise, attribute noise and label noise. Recent works, such as [Patrini et al., 2017], have evidenced that noisy inputs hurt the generalization capability of neural networks. Moreover, noise in a subset of the graph data can easily propagate through the graph topology to corrupt the remaining nodes in the graph data. Nodes that are corrupted by noise or falsely labeled would adversely affect the representation learning of themselves and their neighbors.

While manual data cleaning and labeling could be remedies to the consequence of noise, they are expensive processes and difficult to scale, thus not able to handle almost infinite amount of noisy data online. Therefore, it is crucial to design a robust GNN encoder that could make use of noisy training data while circumventing the adverse effect of noise. In this paper, we propose a novel GCL encoder termed Low-Rank Graph Contrastive Learning (LR-GCL) to improve the robustness and the generalization capabilities of node representations for GNNs.

## 1 INTRODUCTION

Graph Neural Networks (GNNs) have become popular tools for node representation learning in recent years [Kipf and

### 1.1 CONTRIBUTIONS

Our contributions are as follows.

First, we present a novel and provable GCL encoder termed

Low-Rank Graph Contrastive Learning (LR-GCL). Our algorithm is inspired by the low frequency property illustrated in Figure 1. That is, the low-rank projection of the ground truth clean labels possesses the majority of the information of the clean labels, and projection of the label noise is mostly uniform over all the eigenvectors of a kernel matrix used in classification. Inspired by this observation, LR-GCL adds the truncated nuclear norm as a low-rank regularization term in the loss function of the regular prototypical graph contrastive learning. As a result, the features produced by LR-GCL tend to be low-rank, and such low-rank features are the input to the linear transductive classification algorithm. We provide a novel generalization bound for the test loss on the unlabeled data, and our bound is among the first few works which exhibit the advantage of learning with low-rank features for transductive classification with the presence of noise.

Second, we provide strong theoretical guarantee on the generalization capability of the linear transductive algorithm with the low-rank features produced by LR-GCL as the input. Extensive experimental results on popular graph datasets evidence the advantage of LR-GCL over competing methods for node classification on noisy graph data.

## 2 RELATED WORKS

### 2.1 GRAPH NEURAL NETWORKS

Graph neural networks (GNNs) have recently become popular tools for node representation learning. Given the difference in the convolution domain, current GNNs fall into two classes. The first class features spectral convolution [Bruna et al., 2014, Kipf and Welling, 2017], and the second class [Hamilton et al., 2017, Veličković et al., 2017, Xu et al., 2019] generates node representations by sampling and propagating features from their neighborhood. To learn node representation without node labels, contrastive learning has recently been applied to the training of GNNs [Suresh et al., 2021, Thakoor et al., 2021, Wang et al., 2022, Lee et al., 2022, Feng et al., 2022a, Zhang et al., 2023, Lin et al., 2023]. Most proposed graph contrastive learning methods [Veličković et al., 2019, Sun et al., 2019, Hu et al., 2019, Jiao et al., 2020, Peng et al., 2020, You et al., 2021, Jin et al., 2021, Mo et al., 2022] create multiple views of the unlabeled input graph and maximize agreement between the node representations of these views. For example, SFA [Zhang et al., 2023] manipulates the spectrum of the node embeddings to construct augmented views in graph contrastive learning. In addition to constructing node-wise augmented views, recent works [Xu et al., 2021, Guo et al., 2022, Li et al., 2021] propose to perform contrastive learning between node representations and semantic prototype representations [Snell et al., 2017, Arik and Pfister, 2020, Allen et al., 2019, Xu et al., 2020] to encode the global semantics information.

However, as pointed out by [Dai et al., 2021], the perfor-

mance of GNNs can be easily degraded by noisy training data [NT et al., 2019]. Moreover, the adverse effects of noise in a subset of nodes can be exaggerated by being propagated to the remaining nodes through the network structure, exacerbating the negative impact of noise. Unlike previous GCL methods, we propose using contrastive learning to train GNN encoders that are robust to noise existing in the labels and attributes of nodes.

### 2.2 EXISTING METHODS HANDING NOISY DATA

Previous works [Zhang et al., 2021] have shown that deep neural networks usually generalize badly when trained on input with noise. Existing literature on robust learning mostly fall into two categories. The first category [Patrini et al., 2017, Goldberger and Ben-Reuven, 2016] mitigates the effects of noisy inputs by correcting the computation of loss function, known as loss corruption. The second category aims to select clean samples from noisy inputs for the training [Malach and Shalev-Shwartz, 2017, Jiang et al., 2018, Yu et al., 2019, Li et al., 2020, Han et al., 2018], known as sample selection. To improve the performance of GNNs on graph data with noise, NRGNN [Dai et al., 2021] first introduces a graph edge predictor to predict missing links for connecting unlabeled nodes with labeled nodes. RTGNN [Qian et al., 2022] trains a robust GNN classifier with scarce and noisy node labels. It first classifies labeled nodes into clean and noisy ones and adopts reinforcement supervision to correct noisy labels. To improve the robustness of the node classifier on the dynamic graph, GraphSS [Zhuang and Al Hasan, 2022] proposes to generalize noisy supervision as a kind of self-supervised learning method, which regards the noisy labels, including both manual-annotated labels and auto-generated labels, as one kind of self-information for each node. Different from previous works, we aim to improve the robustness of GNN encoders for node classification by applying low-rank regularization during the training of the transductive classifier.

## 3 PROBLEM SETUP

### 3.1 NOTATIONS

An attributed graph consisting of  $N$  nodes is formally represented by  $\mathcal{G} = (\mathcal{V}, \mathcal{E}, \mathbf{X})$ , where  $\mathcal{V} = \{v_1, v_2, \dots, v_N\}$  and  $\mathcal{E} \subseteq \mathcal{V} \times \mathcal{V}$  denote the set of nodes and edges respectively.  $\mathbf{X} \in \mathbb{R}^{N \times D}$  are the node attributes, and the attributes of each node is in  $\mathbb{R}^D$ . Let  $\mathbf{A} \in \{0, 1\}^{N \times N}$  be the adjacency matrix of graph  $\mathcal{G}$ , with  $\mathbf{A}_{ij} = 1$  if and only if  $(v_i, v_j) \in \mathcal{E}$ .  $\hat{\mathbf{A}} = \mathbf{A} + \mathbf{I}$  denotes the adjacency matrix for a graph with self-loops added.  $\mathbf{D}$  denotes the diagonal degree matrix of  $\hat{\mathbf{A}}$ .  $[n]$  denotes all the natural numbers between 1 and  $N$  inclusively.  $\mathcal{L}$  is a subset of  $[N]$  of size  $m$ , and  $\mathcal{U}$  is a subset of  $[N] \setminus \mathcal{L}$  and  $|\mathcal{U}| = u$ . Let  $\mathcal{V}_{\mathcal{L}}$  and  $\mathcal{V}_{\mathcal{U}}$  denote the set of labeled nodes and unlabeled test nodes respectively, and

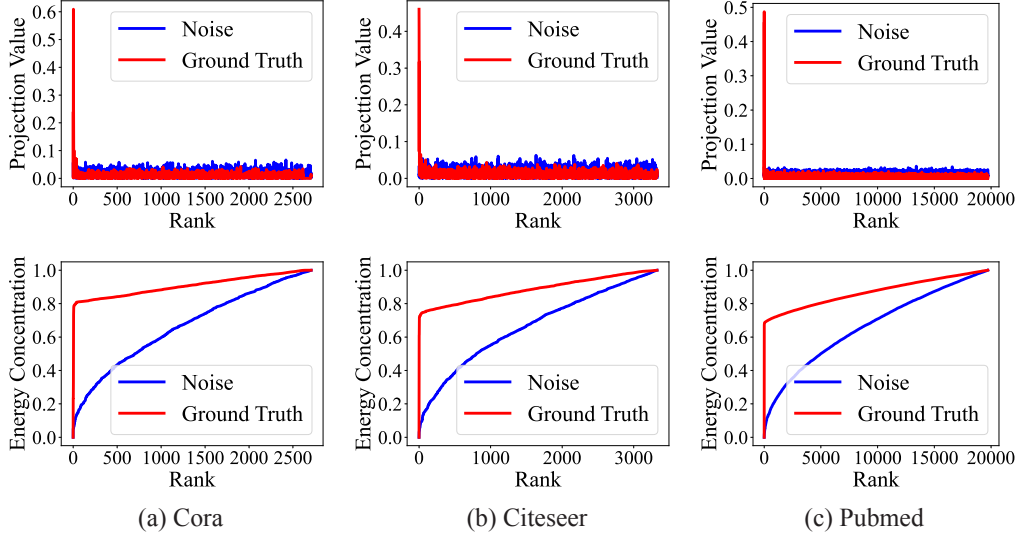


Figure 1: Eigen-projection (first row) and signal concentration ratio (second row) on Cora, Citeseer, and Pubmed. To compute the eigen-projection, we first calculate the eigenvectors  $\mathbf{U}$  of the feature gram matrix  $\mathbf{K} = \mathbf{H}\mathbf{H}^\top$ , then the eigen-projection value is computed by  $\mathbf{p} = \frac{1}{C} \sum_{c=1}^C \frac{\|\mathbf{U}^\top \tilde{\mathbf{Y}}^{(c)}\|_2^2}{\|\tilde{\mathbf{Y}}^{(c)}\|_2^2} \in \mathbb{R}^N$ , where  $C$  is the number of classes, and  $\tilde{\mathbf{Y}} \in \{0, 1\}^{N \times C}$  is the one-hot clean labels of all the nodes,  $\tilde{\mathbf{Y}}^{(c)}$  is the  $c$ -th column of  $\tilde{\mathbf{Y}}$ . With the presence of label noise  $\mathbf{N} \in \mathbb{R}^{N \times C}$ , the observed label matrix is  $\mathbf{Y} = \tilde{\mathbf{Y}} + \mathbf{N}$ . The eigen-projection  $\mathbf{p}_r$  for  $r \in [N]$  reflects the amount of the signal projected onto the  $r$ -th eigenvector of  $\mathbf{K}$ , and the signal concentration ratio of a rank  $r$  reflects the proportion of signal projected onto the top  $r$  eigenvectors of  $\mathbf{K}$ . The signal concentration ratio for rank  $r$  is computed by  $\|\mathbf{p}^{(1:r)}\|_2$ , where  $\mathbf{p}^{(1:r)}$  contains the first  $r$  elements of  $\mathbf{p}$ . It is observed from the red curves in the first row that the projection of the ground truth clean labels mostly concentrates on the top eigenvectors of  $\mathbf{K}$ . On the other hand, the projection of label noise, computed by  $\frac{1}{C} \sum_{c=1}^C \frac{\|\mathbf{U}^\top \mathbf{N}^{(c)}\|_2^2}{\|\mathbf{Y}^{(c)}\|_2^2} \in \mathbb{R}^N$ , is relatively uniform over all the eigenvectors, as illustrated by the blue curves in the first row. For example, by the rank  $r = 0.2 \min\{N, d\}$ , the signal concentration ratio of  $\tilde{\mathbf{Y}}$  for Cora, Citeseer, and Pubmed are 0.844, 0.809, and 0.784 respectively. We refer to such property as the **low frequency property**, which suggests that we can learn a low-rank portion of the observed label  $\mathbf{Y}$  which covers most information in the ground truth clean label while only learning a small portion of the label noise. Figure 3 in the supplementary further illustrates the low frequency property on more datasets.

$|\mathcal{V}_\mathcal{L}| = m$ ,  $|\mathcal{V}_\mathcal{U}| = u$ . Note that  $m + u \leq N$ , and it is not necessary that  $m + u = N$  because there are usually validation nodes other than the labeled nodes and unlabeled test nodes. Let  $\mathbf{u} \in \mathbb{R}^N$  be a vector, we use  $[\mathbf{u}]_{\mathcal{A}}$  to denote a vector formed by elements of  $\mathbf{u}$  with indices in  $\mathcal{L}$  for  $\mathcal{A} \subseteq [N]$ . If  $\mathbf{u}$  is a matrix, then  $[\mathbf{u}]_{\mathcal{A}}$  denotes a submatrix formed by rows of  $\mathbf{u}$  with row indices in  $\mathcal{A}$ .  $\|\cdot\|_F$  denotes the Frobenius norm of a matrix, and  $\|\cdot\|_p$  denotes the  $p$ -norm of a vector.

### 3.2 GRAPH CONVOLUTION NETWORK (GCN)

To learn the node representation from the attributes  $\mathbf{X}$  and the graph structure  $\mathbf{A}$ , one simple yet effective neural network model is Graph Convolution Network (GCN). GCN is originally proposed for semi-supervised node classification, which consists of two graph convolution layers. In our work, we use GCN as the backbone of the proposed LR-GCL, which is the GCL encoder, to obtain node representation  $\mathbf{H} \in \mathbb{R}^{N \times d}$ , where the  $i$ -th row of  $\mathbf{H}$  is the

node representation of  $v_i$ . In this manner, the output of LR-GCL is  $\mathbf{H} = g(\mathbf{X}, \mathbf{A}) = \sigma(\hat{\mathbf{A}}\sigma(\hat{\mathbf{A}}\mathbf{X}\tilde{\mathbf{W}}^{(0)})\tilde{\mathbf{W}}^{(1)})$ , where  $\hat{\mathbf{A}} = \tilde{\mathbf{D}}^{-1/2}\tilde{\mathbf{A}}\tilde{\mathbf{D}}^{-1/2}$ ,  $\tilde{\mathbf{W}}^{(0)}$  and  $\tilde{\mathbf{W}}^{(1)}$  are the weight matrices, and  $\sigma$  is the activation function ReLU. The robust and low-rank node representations produced by the LR-GCL are used to perform transductive node classification by a linear classifier. LR-GCL and the linear transductive node classification algorithm are detailed in Section 4.

### 3.3 PROBLEM DESCRIPTION

Noise usually exists in the input node attributes or labels of real-world graphs, which degrades the quality of the node representation obtained by common GCL encoders and affects the performance of the classifier trained on such representations. We aim to obtain node representations robust to noise in two cases, where noise is present in either the labels of  $\mathcal{V}_\mathcal{L}$  or in the input node attributes  $\mathbf{X}$ . That is, we consider either noisy label or noisy input node attributes.

The goal of LR-GCL is to learn low-rank node representations by  $\mathbf{H} = g(\mathbf{X}, \mathbf{A})$  such that the node representations  $\{\mathbf{h}_i\}_{i=1}^N$  are robust to noise in the above two cases, where  $g(\cdot)$  is the LR-GCL encoder. In our work,  $g$  is a two-layer GCN introduced in Section 3.2. The low-rank node representations by LR-GCL,  $\mathbf{H} = \{\mathbf{h}_1; \mathbf{h}_2; \dots; \mathbf{h}_N\} \in \mathbb{R}^{N \times d}$ , are used for transductive node classification by a linear classifier. In transductive node classification, a linear transductive classifier is trained on  $\mathcal{V}_{\mathcal{L}}$ , and then the classifier predicts the labels of the unlabeled test nodes in  $\mathcal{V}_{\mathcal{U}}$ .

## 4 METHODS

### 4.1 LOW-RANK GCL: LOW-RANK GRAPH CONTRASTIVE LEARNING

**Preliminary of Prototypical GCL.** The general node representation learning aims to train an encoder  $g(\cdot)$ , which is a two-layer Graph Convolution Neural Network (GCN) [Kipf and Welling, 2017], to generate discriminative node representations. In our work, we adopt contrastive learning to train the GCL encoder  $g(\cdot)$ . To perform contrastive learning, two different views,  $G^1 = (\mathbf{X}^1, \mathbf{A}^1)$  and  $G^2 = (\mathbf{X}^2, \mathbf{A}^2)$ , are generated by node dropping, edge perturbation, and attribute masking. The representation of two generated views are denoted as  $\mathbf{H}^1 = g(\mathbf{X}^1, \mathbf{A}^1)$  and  $\mathbf{H}^2 = g(\mathbf{X}^2, \mathbf{A}^2)$ , with  $\mathbf{H}_i^1$  and  $\mathbf{H}_i^2$  being the  $i$ -th row of  $\mathbf{H}^1$  and  $\mathbf{H}^2$ , respectively. It is preferred that the mutual information between  $\mathbf{H}^1$  and  $\mathbf{H}^2$  is maximized. For computational reason, its lower bound is usually used as the objective for contrastive learning. We use InfoNCE [Li et al., 2021] as our node-wise contrastive loss. In addition to the node-wise contrastive learning, we also adopt prototypical contrastive learning [Li et al., 2021] to capture semantic information in the node representations, which is interpreted as maximizing the mutual information between node representation and a set of estimated cluster prototypes  $\{\mathbf{c}_1, \dots, \mathbf{c}_K\}$ . Following [Li et al., 2021, Snell et al., 2017], we use  $K$ -means to cluster the node representations  $\{\mathbf{h}_i\}_{i=1}^N$  into  $K$  clusters and take the clustering centroid of the  $k$ -th cluster as the  $k$ -th prototype  $\mathbf{c}_k = \frac{1}{|S_k|} \sum_{\mathbf{h}_i \in S_k} \mathbf{h}_i$  for all  $k \in [K]$ . The loss function of Prototypical GCL is comprised of two terms,  $\mathcal{L}_{node}$ , the loss function for node-wise contrastive learning, and  $\mathcal{L}_{proto}$ , the prototypical contrastive learning loss, which are presented below:

$$\begin{aligned} \mathcal{L}_{node} &= -\frac{1}{N} \sum_{i=1}^N \log \frac{s(\mathbf{H}_i^1, \mathbf{H}_i^2)}{s(\mathbf{H}_i^1, \mathbf{H}_i^2) + \sum_{j=1}^N s(\mathbf{H}_i^1, \mathbf{H}_j^2)}, \\ \mathcal{L}_{proto} &= -\frac{1}{N} \sum_{i=1}^N \log \frac{\exp(\mathbf{H}_i \cdot \mathbf{c}_k / \tau)}{\sum_{k=1}^K \exp(\mathbf{H}_i \cdot \mathbf{c}_k / \tau)}. \end{aligned} \quad (1)$$

Here  $s(\mathbf{H}_i^1, \mathbf{H}_i^2)$  is the cosine similarity between two node representations,  $\mathbf{H}_i^1$  and  $\mathbf{H}_i^2$ .

**LR-GCL: Low-Rank Graph Contrastive Learning.** LR-GCL aims to improve the robustness and generalization capability of the node representations of Prototypical GCL

by enforcing the learned feature kernel to be low-rank. The gram matrix  $\mathbf{K}$  of the node representations  $\mathbf{H} \in \mathbb{R}^{N \times d}$  is calculated by  $\mathbf{K} = \mathbf{H}^\top \mathbf{H} \in \mathbb{R}^{N \times N}$ . Let  $\{\hat{\lambda}_i\}_{i=1}^n$  with  $\hat{\lambda}_1 \geq \hat{\lambda}_2 \geq \dots \geq \hat{\lambda}_{\min\{N,d\}} \geq \hat{\lambda}_{\min\{N,d\}+1} = \dots = 0$  be the eigenvalues of  $\mathbf{K}$ . In order to encourage the features  $\mathbf{H}$  or the gram matrix  $\mathbf{H}^\top \mathbf{H}$  to be low-rank, we explicitly add the truncated nuclear norm  $\|\mathbf{H}\|_{r_0+1} := \sum_{r=r_0}^n \hat{\lambda}_i$  to the loss function of prototypical GCL. The starting rank  $r_0 < \min(n, d)$  is the rank of the features  $\mathbf{H}$  we aim to obtain with the LR-GCL encoder, that is, if  $\|\mathbf{H}\|_{r_0} = 0$ , then  $\text{rank}(\mathbf{H}) = r_0$ . Therefore, the overall loss function of LR-GCL is

$$\mathcal{L}_{\text{LR-GCL}} = \mathcal{L}_{\text{node}} + \mathcal{L}_{\text{proto}} + \tau \|\mathbf{H}\|_{r_0}, \quad (2)$$

where  $\tau > 0$  is the weighting parameter for the truncated nuclear norm  $\|\mathbf{H}\|_{r_0}$ . We summarize the training algorithm for the LR-GCL encoder in Algorithm 1. After finishing the training, we calculate the low-rank node feature by  $\mathbf{H}^{(r_0)} = g(\mathbf{A}, \mathbf{X})$ .

**Motivation of Learning Low-Rank Features.** Let  $\tilde{\mathbf{Y}} \in \mathbb{R}^{N \times C}$  be the ground truth clean label matrix without noise. By the low frequency property illustrated in Figure 1, the projection of  $\tilde{\mathbf{Y}}$  on the top  $r$  eigenvectors of  $\mathbf{K}$  with a small rank  $r$ , such as  $r = 0.2N$ , covers the majority of the information in  $\tilde{\mathbf{Y}}$ . On the other hand, the projection of the label noise  $\mathbf{N}$  are distributed mostly uniform across all the eigenvectors. This observation motivates low-rank features  $\mathbf{H}$  or equivalently, the low-rank gram matrix  $\mathbf{K}$ . This is because the low-rank part of the feature matrix  $\mathbf{H}$  or the gram matrix  $\mathbf{K}$  covers the dominant information in the ground truth label  $\tilde{\mathbf{Y}}$  while learning only a small portion of the label noise. Moreover, we remark that the regularization term  $\|\mathbf{H}\|_{r_0}$  in the loss function (2) of LR-GCL is also theoretically motivated by the sharp upper bound for the test loss using a linear transductive classifier, presented as (10) in Theorem 4.1. A smaller  $\|\mathbf{H}\|_{r_0}$  renders a smaller upper bound for the test loss, which ensures better generalization capability of the linear transductive classifier to be introduced in the next subsection.

### 4.2 TRANSDUCTIVE NODE CLASSIFICATION

In this section, we introduce a simple yet standard linear transductive node classification algorithm using the low-rank node representations  $\mathbf{H} \in \mathbb{R}^{N \times d}$  produced by the LR-GCL encoder. We present strong theoretical result on the generalization bound for the test loss for our low-rank transductive algorithm with the presence of label noise.

We first give basic notations for our algorithm. Let  $\mathbf{y}_i \in \mathbb{R}^C$  be the observed one-hot class label vector for node  $v_i$  for all  $i \in [N]$ , and define  $\mathbf{Y} := [\mathbf{y}_1; \mathbf{y}_2; \dots; \mathbf{y}_N] \in \mathbb{R}^{N \times C}$  be the observed label matrix which may contain label noise  $\mathbf{N} \in \mathbb{R}^{N \times C}$ . We define  $\mathbf{F}(\mathbf{W}) = \mathbf{H}\mathbf{W}$  as the linear output



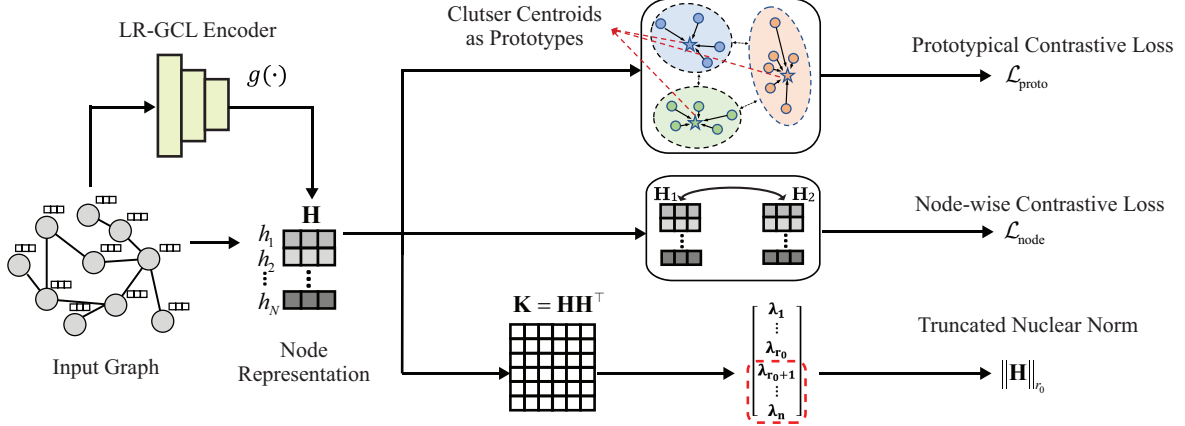


Figure 2: Illustration of the LR-GCL framework.

---

**Algorithm 1** Low-Rank Graph Contrastive Learning (LR-GCL)

---

**Input:** The input attribute matrix  $\mathbf{X}$ , adjacency matrix  $\mathbf{A}$ , and the training epochs  $t_{\max}$ .

**Output:** The parameters of LR-GCL encoder  $g$

- 1: Initialize the parameter of LR-GCL encoder  $g$
  - 2: **for**  $t \leftarrow 1$  to  $t_{\max}$  **do**
  - 3: Calculate node representations by  $\mathbf{H} = g(\mathbf{X}, \mathbf{A})$ , generate augmented views  $G^1, G^2$ , and calculate node representations  $\mathbf{H}^1 = g(\mathbf{X}^1, \mathbf{A}^1)$  and  $\mathbf{H}^2 = g(\mathbf{X}^2, \mathbf{A}^2)$
  - 4: Cluster node representations  $\{\mathbf{h}_i\}_{i=1}^n$  into  $K$  clusters  $\{S_k\}_{k=1}^K$  with  $K$ -means clustering
  - 5: Update the prototype  $\mathbf{c}_k$  as the centroid of  $S_k$  by  $\mathbf{c}_k = \frac{1}{|S_k|} \sum_{\mathbf{h}_i \in S_k} \mathbf{h}_i$  for all  $k \in [K]$
  - 6: Calculate the eigenvalues  $\{\lambda_i\}_{i=1}^N$  of the feature kernel  $\mathbf{H}^\top \mathbf{H}$
  - 7: Update the parameters of LR-GCL encoder  $g$  by one step of gradient descent on the loss  $\mathcal{L}_{rep}$
  - 8: **end for**
  - 9: **return** The LR-GCL encoder  $g$
- 

of the transductive classifier with  $\mathbf{W} \in \mathbb{R}^{d \times C}$  being the weight matrix for the classifier. Our transductive classifier uses  $\text{softmax}(\mathbf{F}(\mathbf{W})) \in \mathbb{R}^{N \times C}$  for prediction of the labels of the test nodes. We train the transductive classifier by minimizing the regular cross-entropy on the labeled nodes via

$$\min_{\mathbf{W}} L(\mathbf{W}) = \frac{1}{m} \sum_{v_i \in \mathcal{V}_{\mathcal{L}}} \text{KL}(\mathbf{y}_i, [\text{softmax}(\mathbf{H}\mathbf{W})]_i), \quad (3)$$

where  $\text{KL}$  is the KL divergence between the label  $\mathbf{y}_i$  and the softmax of the classifier output at node  $v_i$ . We use a regular gradient descent to optimize (3) with a learning rate  $\eta \in (0, \frac{1}{\lambda_1})$ . We define a matrix  $\bar{\mathbf{Y}}(r_0) \in \mathbb{R}^{N \times C}$  as the orthogonal projection of  $\mathbf{Y}$  onto the top- $r_0$  eigenvectors of  $\mathbf{K}$ , that is,  $\bar{\mathbf{Y}}(r_0) = \mathbf{U}^{(r_0)} (\mathbf{U}^{(r_0)})^\top \mathbf{Y}$ , where  $\mathbf{U}^{(r_0)} \in \mathbb{R}^{N \times r_0}$  is the matrix formed by the eigenvectors of  $\mathbf{K}$  corresponding to the top- $r_0$  eigenvalues of  $\mathbf{K}$ .  $\mathbf{W}$  is initialized by  $\mathbf{W}^{(0)} = \mathbf{0}$ ,

and at the  $t$ -th iteration of gradient descent for  $t \geq 1$ ,  $\mathbf{W}$  is updated by  $\mathbf{W}^{(t)} = \mathbf{W}^{(t-1)} - \eta \nabla_{\mathbf{W}} L(\mathbf{W})|_{\mathbf{W}=\mathbf{W}^{(t-1)}}$ .

Define  $\mathbf{F}(\mathbf{W}, t) := \mathbf{H}\mathbf{W}^{(t)}$  as the output of the classifier after the  $t$ -th iteration of gradient descent for  $t \geq 1$ . We have the following theoretical result on the loss of the unlabeled test nodes  $\mathcal{V}_{\mathcal{U}}$  measured by the gap between  $\mathbf{F}(\mathbf{W}, t)$  and  $\bar{\mathbf{Y}}(r_0)$  when using the low-rank feature  $\mathbf{H}$  with  $r_0 \in [n]$ .

**Theorem 4.1.** Let  $m \geq cN$  for a constant  $c \in (0, 1)$ , and  $r_0 \in [n]$ . Assume that a set  $\mathcal{L}$  with  $|\mathcal{L}| = m$  is sampled uniformly without replacement from  $[N]$ , and a set  $\mathcal{U}$  with  $|\mathcal{U}| = u$  are sampled uniformly without replacement from  $[N] \setminus \mathcal{L}$  and  $m + u \leq N$ . Then for every  $x > 0$ , with probability at least  $1 - \exp(-x)$ , after the  $t$ -th iteration of gradient descent for all  $t \geq 1$ , we have

$$\begin{aligned} \mathcal{U}_{\text{test}}(t) &:= \frac{1}{u} \|\mathbf{F}(\mathbf{W}, t) - \mathbf{Y}\|_{\mathcal{U}}^2 \\ &\leq \frac{c_0}{m} \|(\mathbf{I}_N - \eta \mathbf{K})^t \mathbf{Y}\|_{\mathcal{F}} + c_1 r_0 \left( \frac{1}{u} + \frac{1}{m} \right) \\ &\quad + \left( \sqrt{\frac{\|\mathbf{H}\|_{r_0}}{u}} + \sqrt{\frac{\|\mathbf{H}\|_{r_0}}{m}} \right) + \frac{c_2 x}{u}, \end{aligned} \quad (4)$$

where  $c_0, c_1, c_2$  are positive numbers depending on  $\mathbf{U}$ ,  $\{\hat{\lambda}_i\}_{i=1}^{r_0}$ , and  $\tau_0$  with  $\tau_0^2 = \max_{i \in [N]} \mathbf{K}_{ii}$ .

This theorem is proved in Section A of the supplementary. It is noted that  $\frac{1}{u} \|\mathbf{F}(\mathbf{W}, t) - \bar{\mathbf{Y}}(r_0)\|_{\mathcal{U}}^2$  is the test loss of the unlabeled nodes measured by the distance between the classifier output  $\mathbf{F}(\mathbf{W}, t)$  and  $b\mathbf{Y}$ . We remark that the truncated nuclear norm  $\|\mathbf{H}\|_{r_0}$  appears on the RHS of the upper bound (10), theoretically justifying why we learn the low-rank features  $\mathbf{H}$  of the LR-GCL by adding the  $\|\mathbf{H}\|_{r_0}$  to the loss of our LR-GCL. Moreover, when the low frequency property holds, which is always the case as demonstrated by Figure 1 and Figure 3 in the supplementary,  $\|(\mathbf{I}_N - \eta \mathbf{K})^t \mathbf{Y}\|_{\mathcal{F}}$  would be very small with enough iteration number  $t$ .

In our empirical study in the next section, we search for the rank  $r_0$  for the truncated nuclear norm by standard cross-validation for all the graph data sets. In Table 3 of our experimental results, it is observed that the best rank  $r_0$  is always between  $0.1 \min\{N, d\}$  and  $0.3 \min\{N, d\}$ . The overall framework of LR-GCL is illustrated in Figure 2.

## 5 EXPERIMENTS

### 5.1 EXPERIMENTAL SETTINGS

In our experiment, we adopt eight widely used graph benchmark datasets, namely Cora, Citeseer, PubMed [Sen et al., 2008], Coauthor CS, ogbn-arxiv [Hu et al., 2020], Wiki-CS [Mernyei and Cangea, 2020], Amazon-Computers, and Amazon-Photos [Shchur et al., 2018] for the evaluation in node classification. Details of the datasets are deferred in Section 5.2 of the supplementary. Due to the fact that all public benchmark graph datasets do not come with corrupted labels or attribute noise, we manually inject noise into public datasets to evaluate our algorithm. We follow the commonly used label noise generation methods from the existing work [Han et al., 2020, Dai et al., 2022, Qian et al., 2022] to inject label noise. We generate noisy labels over all classes in two types: (1) Symmetric, where nodes from each class is flipped to other classes with a uniform random probability; (2) Asymmetric, where mislabeling only occurs between similar classes. The percentage of nodes with flipped labels is defined as the label noise level in our experiments. To evaluate the performance of our method with attribute noise, we randomly shuffle a certain percentage of input attributes for each node following [Ding et al., 2022]. The percentage of shuffled attributes is defined as the attribute noise level in our experiments.

**Tuning  $r_0, \tau$  by Cross-Validation.** We tune the rank  $r_0$  and the weight for the truncated nuclear loss  $\tau$  by standard cross-validation on each dataset. Let  $r_0 = \lceil \gamma \min\{N, d\} \rceil$  where  $\gamma$  is the rank ratio. We select the values of  $\gamma$  and  $\tau$  by performing 5-fold cross-validation on 20% of the training data in each dataset. The value of  $\gamma$  is selected from  $\{0.1, 0.2, 0.3, 0.4, 0.5, 0.6, 0.7, 0.8, 0.9\}$ . The value of  $\tau$  is selected from  $\{0.05, 0.1, 0.15, 0.2, 0.25, 0.3, 0.35, 0.4, 0.45, 0.5\}$ . The selected values on each dataset are shown in Table 3.

### 5.2 DATASETS

We evaluate our method on eight public benchmarks that are widely used for node representation learning, namely Cora, Citeseer, PubMed [Sen et al., 2008], Coauthor CS, ogbn-arxiv [Hu et al., 2020], Wiki-CS [Mernyei and Cangea, 2020], Amazon-Computers, and Amazon-Photos [Shchur et al., 2018]. Cora, Citeseer, and PubMed are the three most widely used citation networks. Coauthor CS is a

co-authorship graph. The ogbn-arxiv is a directed citation graph. Wiki-CS is a hyperlink networks of computer science articles. Amazon-Computers and Amazon-Photos are co-purchase networks of products selling on Amazon.com. We summarize the statistics of all the datasets in Table 4. For all our experiments, we follow the default separation [Shchur et al., 2018, Mernyei and Cangea, 2020, Hu et al., 2020] of training, validation, and test sets on each benchmark.

### 5.3 NODE CLASSIFICATION

**Compared Methods.** We compare LR-GCL against semi-supervised node representation learning methods, GCN [Kipf and Welling, 2017], GCE [Zhang and Sabuncu, 2018], S<sup>2</sup>GC [Zhu and Koniusz, 2020], and GRAND+ [Feng et al., 2022b]. Furthermore, we include two baseline methods for node classification with label noise, which are NRGNN [Dai et al., 2021] and RTGNN [Qian et al., 2022]. We also compare LR-GCL against state-of-the-art GCL methods, including GraphCL [You et al., 2020], MERIT [Jin et al., 2021], SUGRL [Mo et al., 2022], Jo-SRC [Yao et al., 2021], Sel-CL [Li et al., 2022], and SFA [Zhang et al., 2023]. Among the compared contrastive learning methods, Jo-SRC and Sel-CL are specifically designed for robust learning. SFA is a method that aims to improve the performance of contrastive learning with spectral augmentation. We include details of compared methods in Section B.1 of the supplementary.

#### Experimental Results.

We first compare LR-GCL against competing methods for semi-supervised or transductive node classification on input with two types of label noise. To show the robustness of LR-GCL against label noise, we perform the experiments on graphs injected with different levels of label noise ranging from 40% to 80% with a step of 20%. We follow the widely used semi-supervised setting [Kipf and Welling, 2017] for node classification. In LR-GCL, we train a transductive classifier for node classification. Previous GCL methods, including MERIT, SUGRL, and SFA, train a linear layer for inductive classification on top of the node representations learned by contrastive learning without using test data in training. Because LR-GCL is a transductive classifier, for fair comparisons, we also train the compared GCL baselines with the same transductive classifier as that for LR-GCL and a two-layer GCN transductive classifier. The results with different types of classifiers are deferred in Section C.2 of the supplementary. For all the baselines in our experiments which perform inductive classification when predicting the labels, we report their best results among using their original inductive classifier and two types of transductive classifiers: the same transductive classifier as that for LR-GCL and a two-layer GCN transductive classifier.

Results on Cora, Citeseer, PubMed, Coauthor-CS, and ogbn-

Table 1: Performance comparison for node classification on Cora, Citeseer, PubMed, and Wiki-CS with asymmetric label noise, symmetric label noise, and attribute noise.

Dataset	Methods	Noise Level											
		0			40			60			80		
		-	Asymmetric	Symmetric	Attribute	Asymmetric	Symmetric	Attribute	Asymmetric	Symmetric	Attribute		
Cora	GCN	0.815±0.005	0.547±0.015	0.636±0.007	0.639±0.008	0.405±0.014	0.517±0.010	0.439±0.012	0.265±0.012	0.354±0.014	0.317±0.013		
	S <sup>2</sup> GC	0.835±0.002	0.569±0.007	0.664±0.007	0.661±0.007	0.422±0.010	0.535±0.010	0.454±0.011	0.279±0.014	0.366±0.014	0.320±0.013		
	GCE	0.819±0.004	0.573±0.011	0.652±0.008	0.650±0.014	0.449±0.011	0.509±0.011	0.445±0.015	0.280±0.013	0.353±0.013	0.325±0.015		
	UnionNET	0.820±0.006	0.569±0.014	0.664±0.007	0.653±0.012	0.452±0.010	0.541±0.010	0.450±0.009	0.283±0.014	0.370±0.011	0.320±0.012		
	NRGNN	0.822±0.006	0.571±0.019	0.676±0.007	0.645±0.012	0.470±0.014	0.548±0.014	0.451±0.011	0.282±0.022	0.373±0.012	0.326±0.010		
	RTGNN	0.828±0.003	0.570±0.010	0.682±0.008	0.678±0.011	0.474±0.011	0.555±0.010	0.457±0.009	0.280±0.011	0.386±0.014	0.342±0.016		
	SUGRL	0.834±0.005	0.564±0.011	0.674±0.012	0.675±0.009	0.468±0.011	0.552±0.011	0.452±0.012	0.280±0.012	0.381±0.012	0.338±0.014		
	MERIT	0.831±0.005	0.560±0.008	0.670±0.008	0.671±0.009	0.467±0.013	0.547±0.013	0.450±0.014	0.277±0.013	0.385±0.013	0.335±0.009		
	ARIEL	0.843±0.004	0.573±0.013	0.681±0.010	0.675±0.009	0.471±0.012	0.553±0.012	0.455±0.014	0.284±0.014	0.389±0.013	0.343±0.013		
	SFA	0.839±0.010	0.564±0.011	0.677±0.013	0.676±0.015	0.473±0.014	0.549±0.014	0.457±0.014	0.282±0.016	0.389±0.013	0.344±0.017		
	Sel-Cl	0.828±0.002	0.570±0.010	0.685±0.012	0.676±0.009	0.472±0.013	0.554±0.014	0.455±0.011	0.282±0.017	0.389±0.013	0.341±0.015		
	Jo-SRC	0.825±0.005	0.571±0.006	0.684±0.013	0.679±0.007	0.473±0.011	0.556±0.008	0.458±0.012	0.285±0.013	0.387±0.018	0.345±0.018		
	GRAND+	0.858±0.006	0.570±0.009	0.682±0.007	0.678±0.011	0.472±0.010	0.554±0.008	0.456±0.012	0.284±0.015	0.387±0.015	0.345±0.013		
	LR-GCL	<b>0.858±0.006</b>	<b>0.589±0.011</b>	<b>0.713±0.007</b>	<b>0.695±0.011</b>	<b>0.492±0.011</b>	<b>0.587±0.013</b>	<b>0.477±0.012</b>	<b>0.306±0.012</b>	<b>0.419±0.012</b>	<b>0.363±0.011</b>		
Citeseer	GCN	0.703±0.005	0.475±0.023	0.501±0.013	0.529±0.009	0.351±0.014	0.341±0.014	0.372±0.011	0.291±0.022	0.281±0.019	0.290±0.014		
	S <sup>2</sup> GC	0.736±0.005	0.488±0.013	0.528±0.013	0.553±0.008	0.363±0.012	0.367±0.014	0.390±0.013	0.304±0.024	0.284±0.019	0.288±0.011		
	GCE	0.705±0.004	0.490±0.016	0.512±0.014	0.540±0.014	0.362±0.015	0.352±0.010	0.381±0.009	0.309±0.012	0.285±0.014	0.285±0.011		
	UnionNET	0.706±0.006	0.499±0.015	0.547±0.014	0.545±0.013	0.379±0.013	0.399±0.013	0.379±0.012	0.322±0.021	0.302±0.013	0.290±0.012		
	NRGNN	0.710±0.006	0.498±0.015	0.546±0.015	0.538±0.011	0.382±0.016	0.412±0.016	0.377±0.012	0.336±0.021	0.309±0.018	0.284±0.009		
	RTGNN	0.746±0.008	0.498±0.007	0.556±0.007	0.550±0.012	0.392±0.010	0.424±0.013	0.390±0.014	0.348±0.017	0.308±0.016	0.302±0.011		
	SUGRL	0.730±0.005	0.493±0.011	0.541±0.011	0.544±0.010	0.376±0.009	0.421±0.009	0.388±0.009	0.339±0.010	0.305±0.010	0.300±0.009		
	MERIT	0.740±0.007	0.496±0.012	0.536±0.012	0.542±0.010	0.383±0.011	0.425±0.011	0.387±0.008	0.344±0.014	0.301±0.014	0.295±0.009		
	SFA	0.740±0.011	0.502±0.014	0.532±0.015	0.547±0.013	0.390±0.014	0.433±0.014	0.389±0.012	0.347±0.016	0.312±0.015	0.299±0.013		
	ARIEL	0.727±0.007	0.500±0.008	0.550±0.013	0.548±0.008	0.391±0.009	0.427±0.012	0.389±0.014	0.349±0.014	0.307±0.013	0.299±0.013		
	Sel-Cl	0.725±0.008	0.499±0.012	0.551±0.010	0.549±0.008	0.389±0.011	0.426±0.008	0.391±0.020	0.350±0.018	0.310±0.015	0.300±0.017		
	Jo-SRC	0.730±0.005	0.500±0.013	0.555±0.011	0.551±0.011	0.394±0.013	0.425±0.013	0.393±0.013	0.351±0.013	0.305±0.018	0.303±0.013		
	GRAND+	0.756±0.004	0.497±0.010	0.553±0.010	0.552±0.011	0.390±0.013	0.422±0.013	0.387±0.013	0.348±0.013	0.309±0.014	0.302±0.012		
	LR-GCL	<b>0.757±0.010</b>	<b>0.520±0.013</b>	<b>0.581±0.013</b>	<b>0.570±0.007</b>	<b>0.410±0.014</b>	<b>0.455±0.014</b>	<b>0.406±0.012</b>	<b>0.369±0.012</b>	<b>0.335±0.014</b>	<b>0.318±0.010</b>		
PubMed	GCN	0.790±0.007	0.584±0.022	0.574±0.012	0.595±0.012	0.405±0.025	0.386±0.011	0.488±0.013	0.305±0.022	0.295±0.013	0.423±0.013		
	S <sup>2</sup> GC	0.802±0.005	0.585±0.023	0.589±0.013	0.610±0.009	0.421±0.030	0.401±0.014	0.497±0.012	0.310±0.039	0.290±0.019	0.431±0.010		
	GCE	0.792±0.009	0.589±0.018	0.581±0.011	0.590±0.014	0.430±0.012	0.399±0.012	0.491±0.010	0.311±0.021	0.301±0.011	0.424±0.012		
	UnionNET	0.793±0.008	0.603±0.020	0.620±0.012	0.592±0.012	0.445±0.022	0.424±0.013	0.489±0.015	0.313±0.025	0.327±0.015	0.435±0.009		
	NRGNN	0.797±0.008	0.602±0.022	0.618±0.013	0.603±0.008	0.443±0.012	0.434±0.012	0.499±0.009	0.330±0.023	0.325±0.013	0.433±0.011		
	RTGNN	0.797±0.004	0.610±0.008	0.622±0.010	0.614±0.012	0.455±0.010	0.455±0.011	0.501±0.011	0.335±0.013	0.338±0.017	0.452±0.013		
	SUGRL	0.819±0.005	0.603±0.013	0.615±0.013	0.615±0.010	0.445±0.011	0.441±0.011	0.501±0.007	0.321±0.009	0.321±0.009	0.446±0.010		
	MERIT	0.801±0.004	0.593±0.011	0.612±0.011	0.613±0.011	0.447±0.012	0.443±0.012	0.497±0.009	0.328±0.011	0.323±0.011	0.445±0.009		
	ARIEL	0.800±0.003	0.610±0.013	0.622±0.010	0.615±0.011	0.453±0.012	0.453±0.012	0.502±0.014	0.331±0.014	0.336±0.018	0.457±0.013		
	SFA	0.804±0.010	0.596±0.011	0.615±0.011	0.609±0.011	0.447±0.014	0.446±0.017	0.499±0.014	0.330±0.011	0.327±0.011	0.447±0.014		
	Sel-Cl	0.799±0.005	0.605±0.014	0.625±0.012	0.614±0.012	0.455±0.014	0.449±0.010	0.502±0.008	0.334±0.021	0.332±0.014	0.456±0.014		
	Jo-SRC	0.801±0.005	0.613±0.010	0.624±0.013	0.617±0.013	0.453±0.008	0.455±0.013	0.504±0.013	0.330±0.015	0.334±0.018	0.459±0.018		
	GRAND+	0.845±0.006	0.610±0.011	0.624±0.013	0.617±0.013	0.453±0.008	0.453±0.011	0.503±0.010	0.331±0.014	0.337±0.013	0.458±0.014		
	LR-GCL	<b>0.845±0.009</b>	<b>0.637±0.014</b>	<b>0.645±0.015</b>	<b>0.637±0.011</b>	<b>0.479±0.011</b>	<b>0.484±0.013</b>	<b>0.526±0.011</b>	<b>0.356±0.011</b>	<b>0.360±0.012</b>	<b>0.482±0.014</b>		
Coauthor-CS	GCN	0.918±0.001	0.645±0.009	0.656±0.006	0.702±0.010	0.511±0.013	0.501±0.009	0.531±0.010	0.429±0.022	0.389±0.011	0.415±0.013		
	S <sup>2</sup> GC	0.918±0.001	0.657±0.012	0.663±0.006	0.713±0.010	0.516±0.013	0.514±0.009	0.556±0.009	0.437±0.020	0.396±0.010	0.422±0.012		
	GCE	0.922±0.003	0.662±0.017	0.659±0.007	0.705±0.014	0.515±0.016	0.502±0.007	0.539±0.009	0.443±0.017	0.389±0.012	0.412±0.011		
	UnionNET	0.918±0.002	0.669±0.023	0.671±0.013	0.706±0.012	0.525±0.011	0.529±0.011	0.540±0.012	0.458±0.015	0.401±0.011	0.420±0.007		
	NRGNN	0.919±0.002	0.678±0.014	0.689±0.009	0.705±0.012	0.545±0.021	0.556±0.011	0.546±0.011	0.461±0.012	0.410±0.012	0.417±0.007		
	RTGNN	0.920±0.005	0.678±0.012	0.691±0.009	0.712±0.008	0.559±0.010	0.569±0.011	0.560±0.008	0.455±0.015	0.415±0.015	0.412±0.014		
	SUGRL	0.922±0.005	0.675±0.010	0.695±0.010	0.714±0.006	0.550±0.011	0.560±0.011	0.561±0.007	0.449±0.011	0.411±0.011	0.429±0.008		
	MERIT	0.924±0.004	0.679±0.011	0.689±0.008	0.709±0.005	0.552±0.014	0.562±0.014	0.562±0.011	0.452±0.013	0.403±0.013	0.426±0.005		
	ARIEL	0.925±0.004	0.682±0.011	0.699±0.009	0.712±0.005	0.555±0.011	0.566±0.011	0.556±0.011	0.454±0.014	0.415±0.019	0.427±0.013		
	SFA	0.925±0.009	0.682±0.011	0.690±0.012	0.715±0.012	0.555±0.015	0.567±0.014	0.565±0.013	0.458±0.013	0.402±0.013	0.429±0.015		
	Sel-Cl	0.922±0.008	0.684±0.009	0.694±0.012	0.714±0.010	0.557±0.013	0.568±0.013	0.566±0.010	0.457±0.013	0.412±0.017	0.425±0.009		
	Jo-SRC	0.921±0.005	0.684±0.011	0.695±0.004	0.709±0.007	0.560±0.011	0.566±0.011	0.561±0.009	0.456±0.013	0.410±0.018	0.428±0.010		
	GRAND+	0.927±0.004	0.682±0.011	0.693±0.006	0.715±0.008	0.554±0.008	0.568±0.013	0.557±0.011	0.455±0.012	0.416±0.013	0.428±0.011		
	LR-GCL	<b>0.933±0.006</b>	<b>0.699±0.015</b>	<b>0.721±0.011</b>	<b>0.742±0.015</b>	<b>0.575±0.014</b>	<b>0.595±0.018</b>	<b>0.588±0.015</b>	<b>0.469±0.015</b>	<b>0.389±0.015</b>	<b>0.453±0.017</b>		
ogbn-arxiv	GCN	0.717±0.003	0.401±0.014	0.421±0.014	0.478±0.010	0.336±0.011	0.346±0.021	0.339±0.012	0.286±0.022	0.256±0.010	0.294±0.013		
	S <sup>2</sup> GC	0.712±0.003	0.417±0.017	0.429±0.014	0.492±0.010	0.344±0.016	0.353±0.031	0.343±0.009	0.297±0.023	0.266±0.013	0.284±0.012		
	GCE	0.720±0.004	0.410±0.018	0.428±0.008	0.480±0.014	0.348±0.019	0.344±0.019	0.342±0.015	0.310±0.014	0.260±0.011	0.275±0.015		
	UnionNET	0.724±0.006	0.429±0.021	0.449±0.007	0.485±0.012	0.362±0.018	0.367±0.008	0.340±0.009	0.332±0.019	0.269±0.013	0.280±0.012		
	NRGNN	0.721±0.006	0.449±0.014	0.466±0.009	0.485±0.012	0.371±0.020	0.379±0.008	0.342±0.011	0.330±0.018	0.271±0.018	0.300±0.010		
	RTGNN	0.718±0.004	0.443±0.012	0.464±0.012	0.484±0.014	0.380±0.011	0.384±0.013	0.340±0.017	0.335±0.011	0.285±0.015	0.301±0.006		
	SUGRL	0.693±0.002	0.439±0.010	0.467±0.010	0.480±0.012	0.365±0.013	0.385±0.011	0.341±0.009	0.327±0.011	0.275±0.011	0.295±0.011		
	MERIT	0.717±0.004	0.442±0.009	0.463±0.009	0.483±0.010	0.368±0.011	0.381±0.011	0.341±0.012	0.324±0.012	0.272±0.010	0.304±0.009		

Table 2: Ablation study on the value of rank  $r_0$  in the optimization problem (3) on Cora with different levels of asymmetric and symmetric label noise. The accuracy with the optimal rank is shown in the last row. The accuracy difference against the optimal rank is shown for other ranks.

Rank	Noise Level						
	0	40		60		80	
	-	Asymmetric	Symmetric	Asymmetric	Symmetric	Asymmetric	Symmetric
0.1 min $\{N, d\}$	-0.002	-0.001	-0.002	-0.002	-0.001	-0.001	-0.000
0.2 min $\{N, d\}$	-0.000	-0.000	-0.000	-0.000	-0.000	-0.000	-0.000
0.3 min $\{N, d\}$	-0.000	-0.000	-0.001	-0.002	-0.001	-0.000	-0.001
0.4 min $\{N, d\}$	-0.001	-0.003	-0.002	-0.001	-0.002	-0.002	-0.002
0.5 min $\{N, d\}$	-0.001	-0.002	-0.003	-0.003	-0.003	-0.001	-0.002
0.6 min $\{N, d\}$	-0.003	-0.002	-0.002	-0.003	-0.002	-0.002	-0.003
0.7 min $\{N, d\}$	-0.003	-0.004	-0.003	-0.004	-0.004	-0.004	-0.005
0.8 min $\{N, d\}$	-0.002	-0.005	-0.006	-0.006	-0.006	-0.007	-0.007
0.9 min $\{N, d\}$	-0.004	-0.004	-0.005	-0.007	-0.008	-0.008	-0.006
min $\{N, d\}$	-0.004	-0.004	-0.007	-0.007	-0.008	-0.010	-0.008
optimal	0.858	0.589	0.713	0.492	0.587	0.306	0.419

Table 3: Selected rank ratio  $\gamma$  and truncated nuclear loss’s weight  $\lambda$  for each dataset.

Hyper-parameters	Cora	Citeseer	PubMed	Coauthor CS	ogbn-arxiv	Wiki-CS	Amazon-Computers	Amazon-Photos
$\tau$	0.10	0.10	0.10	0.20	0.10	0.25	0.20	0.20
$\gamma$	0.2	0.2	0.3	0.3	0.4	0.2	0.2	0.3

Table 4: The statistics of the datasets.

Dataset	Nodes	Edges	Features	Classes
<b>Cora</b>	2,708	5,429	1,433	7
<b>CiteSeer</b>	3,327	4,732	3,703	6
<b>PubMed</b>	19,717	44,338	500	3
<b>Coauthor CS</b>	18,333	81,894	6,805	15
<b>ogbn-arxiv</b>	169,343	1,166,243	128	40
<b>Wiki-CS</b>	11,701	215,863	300	10
<b>Amazon-Computers</b>	13,752	245,861	767	10
<b>Amazon-Photos</b>	7,650	119,081	745	8

with a step of 20%. Results on Cora, Citeseer, and Coauthor CS are shown in Table 5 in the supplementary, where we report the means of the accuracy of 10 runs and the standard deviation. The results clearly show that LR-GCL is more robust to attribute noise compared to all the baselines for different noise levels.

**Additional Results and Ablation Studies** We compare the training time of LR-GCL with competing baselines in Table 7 of the supplementary. We also perform ablation study on the value of rank  $r_0$  in the truncated nuclear norm  $\|\mathbf{H}\|_{r_0}$  in the loss function (2) of LR-GCL. It is observed from Table 2 that the performance of our LR-GCL is consistently close to the best performance among all the choices of the rank when  $r_0$  is between  $0.1 \min \{N, d\}$  and  $0.3 \min \{N, d\}$ .

## 6 CONCLUSIONS

In this paper, we propose a novel GCL encoder termed Low-Rank Graph Contrastive Learning (LR-GCL). LR-GCL is a robust GCL encoder which produces low-rank features inspired by the low frequency property of universal graph datasets and the sharp generalization bound for transductive learning. LR-GCL is trained with prototypical GCL with the truncated nuclear norm as the regularization term. We evaluate the performance of LR-GCL with comparison to competing baselines on semi-supervised or transductive node classification, where graph data are corrupted with noise in either the labels for the node attributes. Extensive experimental results demonstrate that LR-GCL generates more robust node representations with better performance than the current state-of-the-art node representation learning methods.

## References

- Kelsey Allen, Evan Shelhamer, Hanul Shin, and Joshua Tenenbaum. Infinite mixture prototypes for few-shot learning. In *International Conference on Machine Learning*, pages 232–241. PMLR, 2019.
- Sercan Ö Arik and Tomas Pfister. Protoattend: Attention-based prototypical learning. *The Journal of Machine Learning Research*, 21(1):8691–8725, 2020.
- Joan Bruna, Wojciech Zaremba, Arthur Szlam, and Yann LeCun. Spectral networks and locally connected networks on graphs. *ICLR*, 2014.



- Enyan Dai, Charu Aggarwal, and Suhang Wang. Nrgnn: Learning a label noise-resistant graph neural network on sparsely and noisily labeled graphs. *SIGKDD*, 2021.
- Enyan Dai, Wei Jin, Hui Liu, and Suhang Wang. Towards robust graph neural networks for noisy graphs with sparse labels. In *Proceedings of the Fifteenth ACM International Conference on Web Search and Data Mining*, pages 181–191, 2022.
- Kaize Ding, Zhe Xu, Hanghang Tong, and Huan Liu. Data augmentation for deep graph learning: A survey. *arXiv preprint arXiv:2202.08235*, 2022.
- Shengyu Feng, Baoyu Jing, Yada Zhu, and Hanghang Tong. Adversarial graph contrastive learning with information regularization. In *Proceedings of the ACM Web Conference 2022*, pages 1362–1371, 2022a.
- Wenzheng Feng, Yuxiao Dong, Tinglin Huang, Ziqi Yin, Xu Cheng, Evgeny Kharlamov, and Jie Tang. Grand+: Scalable graph random neural networks. In *Proceedings of the ACM Web Conference 2022*, pages 3248–3258, 2022b.
- Jacob Goldberger and Ehud Ben-Reuven. Training deep neural-networks using a noise adaptation layer. 2016.
- Yuanfan Guo, Minghao Xu, Jiawen Li, Bingbing Ni, Xuanyu Zhu, Zhenbang Sun, and Yi Xu. Hesc: hierarchical contrastive selective coding. In *Proceedings of the IEEE/CVF Conference on Computer Vision and Pattern Recognition*, pages 9706–9715, 2022.
- Will Hamilton, Zhitaoying Ying, and Jure Leskovec. Inductive representation learning on large graphs. *NeurIPS*, 30, 2017.
- Bo Han, Quanming Yao, Xingrui Yu, Gang Niu, Miao Xu, Weihua Hu, Ivor Tsang, and Masashi Sugiyama. Co-teaching: Robust training of deep neural networks with extremely noisy labels. pages 8536–8546, 2018.
- Bo Han, Quanming Yao, Tongliang Liu, Gang Niu, Ivor W Tsang, James T Kwok, and Masashi Sugiyama. A survey of label-noise representation learning: Past, present and future. *arXiv preprint arXiv:2011.04406*, 2020.
- Weihua Hu, Bowen Liu, Joseph Gomes, Marinka Zitnik, Percy Liang, Vijay Pande, and Jure Leskovec. Strategies for pre-training graph neural networks. *arXiv preprint arXiv:1905.12265*, 2019.
- Weihua Hu, Matthias Fey, Marinka Zitnik, Yuxiao Dong, Hongyu Ren, Bowen Liu, Michele Catasta, and Jure Leskovec. Open graph benchmark: Datasets for machine learning on graphs. In *NeurIPS*, 2020.
- Lu Jiang, Zhengyuan Zhou, Thomas Leung, Li-Jia Li, and Li Fei-Fei. Mentornet: Learning data-driven curriculum for very deep neural networks on corrupted labels. In *International Conference on Machine Learning*, pages 2304–2313. PMLR, 2018.
- Yizhu Jiao, Yun Xiong, Jiawei Zhang, Yao Zhang, Tianqi Zhang, and Yangyong Zhu. Sub-graph contrast for scalable self-supervised graph representation learning. In *2020 IEEE international conference on data mining (ICDM)*, pages 222–231. IEEE, 2020.
- Ming Jin, Yizhen Zheng, Yuan-Fang Li, Chen Gong, Chuan Zhou, and Shirui Pan. Multi-scale contrastive siamese networks for self-supervised graph representation learning. In *The 30th International Joint Conference on Artificial Intelligence (IJCAI)*, 2021.
- Thomas N. Kipf and Max Welling. Semi-supervised classification with graph convolutional networks. In *ICLR*, 2017.
- Namkyeong Lee, Junseok Lee, and Chanyoung Park. Augmentation-free self-supervised learning on graphs. In *Proceedings of the AAAI Conference on Artificial Intelligence*, volume 36, pages 7372–7380, 2022.
- Junnan Li, Richard Socher, and Steven CH Hoi. Dividemix: Learning with noisy labels as semi-supervised learning. *arXiv preprint arXiv:2002.07394*, 2020.
- Junnan Li, Pan Zhou, Caiming Xiong, and Steven C.H. Hoi. Prototypical contrastive learning of unsupervised representations. In *ICLR*, 2021.
- Shikun Li, Xiaobo Xia, Shiming Ge, and Tongliang Liu. Selective-supervised contrastive learning with noisy labels. In *Proceedings of the IEEE/CVF Conference on Computer Vision and Pattern Recognition*, pages 316–325, 2022.
- Lu Lin, Jinghui Chen, and Hongning Wang. Spectral augmentation for self-supervised learning on graphs. *ICLR*, 2023.
- Eran Malach and Shai Shalev-Shwartz. Decoupling “when to update” from “how to update”. In *NeurIPS*, pages 960–970, 2017.
- Péter Mernyei and Cătălina Cangea. Wiki-cs: A wikipedia-based benchmark for graph neural networks. *arXiv preprint arXiv:2007.02901*, 2020.
- Yujie Mo, Liang Peng, Jie Xu, Xiaoshuang Shi, and Xiaofeng Zhu. Simple unsupervised graph representation learning. AAAI, 2022.
- Hoang NT, Choong Jin, and Tsuyoshi Murata. Learning graph neural networks with noisy labels. In *2nd ICLR Learning from Limited Labeled Data (LLD) Workshop*, 2019.

- Giorgio Patrini, Alessandro Rozza, Aditya Krishna Menon, Richard Nock, and Lizhen Qu. Making deep neural networks robust to label noise: A loss correction approach. In *CVPR*, pages 1944–1952, 2017.
- Zhen Peng, Wenbing Huang, Minnan Luo, Qinghua Zheng, Yu Rong, Tingyang Xu, and Junzhou Huang. Graph representation learning via graphical mutual information maximization. In *Proceedings of The Web Conference 2020*, pages 259–270, 2020.
- Siyi Qian, Haochao Ying, Renjun Hu, Jingbo Zhou, Jintai Chen, Danny Z Chen, and Jian Wu. Robust training of graph neural networks via noise governance. *WSDM*, 2022.
- Prithviraj Sen, Galileo Namata, Mustafa Bilgic, Lise Getoor, Brian Gallagher, and Tina Eliassi-Rad. Collective classification in network data. *AI Magazine*, 29(3):93–93, 2008.
- Oleksandr Shchur, Maximilian Mumme, Aleksandar Bojchevski, and Stephan Günnemann. Pitfalls of graph neural network evaluation. *arXiv preprint arXiv:1811.05868*, 2018.
- Jake Snell, Kevin Swersky, and Richard Zemel. Prototypical networks for few-shot learning. *Advances in neural information processing systems*, 30, 2017.
- Fan-Yun Sun, Jordan Hoffman, Vikas Verma, and Jian Tang. Infograph: Unsupervised and semi-supervised graph-level representation learning via mutual information maximization. In *ICLR*, 2019.
- Susheel Suresh, Pan Li, Cong Hao, and Jennifer Neville. Adversarial graph augmentation to improve graph contrastive learning. *Advances in Neural Information Processing Systems*, 34:15920–15933, 2021.
- Shantanu Thakoor, Corentin Tallec, Mohammad Gheshlaghi Azar, Rémi Munos, Petar Veličković, and Michal Valko. Bootstrapped representation learning on graphs. In *ICLR 2021 Workshop on Geometrical and Topological Representation Learning*, 2021.
- Petar Veličković, Guillem Cucurull, Arantxa Casanova, Adriana Romero, Pietro Lio, and Yoshua Bengio. Graph attention networks. *arXiv preprint arXiv:1710.10903*, 2017.
- Petar Veličković, William Fedus, William L. Hamilton, Pietro Liò, Yoshua Bengio, and R Devon Hjelm. Deep graph infomax. In *ICLR*, 2019.
- Haonan Wang, Jieyu Zhang, Qi Zhu, and Wei Huang. Augmentation-free graph contrastive learning with performance guarantee. *arXiv preprint arXiv:2204.04874*, 2022.
- Keyulu Xu, Weihua Hu, Jure Leskovec, and Stefanie Jegelka. How powerful are graph neural networks? *ICLR*, 2019.
- Minghao Xu, Hang Wang, Bingbing Ni, Hongyu Guo, and Jian Tang. Self-supervised graph-level representation learning with local and global structure. In *International Conference on Machine Learning*, pages 11548–11558. PMLR, 2021.
- Wenjia Xu, Yongqin Xian, Jiuniu Wang, Bernt Schiele, and Zeynep Akata. Attribute prototype network for zero-shot learning. *Advances in Neural Information Processing Systems*, 33:21969–21980, 2020.
- Yingzhen Yang. Sharp generalization of transductive learning: A transductive local rademacher complexity approach. 2023. URL <https://arxiv.org/pdf/2309.16858.pdf>.
- Yazhou Yao, Zeren Sun, Chuanyi Zhang, Fumin Shen, Qi Wu, Jian Zhang, and Zhenmin Tang. Jo-src: A contrastive approach for combating noisy labels. In *Proceedings of the IEEE/CVF Conference on Computer Vision and Pattern Recognition*, pages 5192–5201, 2021.
- Yuning You, Tianlong Chen, Yongduo Sui, Ting Chen, Zhangyang Wang, and Yang Shen. Graph contrastive learning with augmentations. *Advances in Neural Information Processing Systems*, 33:5812–5823, 2020.
- Yuning You, Tianlong Chen, Yang Shen, and Zhangyang Wang. Graph contrastive learning automated. In *International Conference on Machine Learning*, pages 12121–12132. PMLR, 2021.
- Xingrui Yu, Bo Han, Jiangchao Yao, Gang Niu, Ivor W Tsang, and Masashi Sugiyama. How does disagreement help generalization against label corruption? 2019.
- Chiyuan Zhang, Samy Bengio, Moritz Hardt, Benjamin Recht, and Oriol Vinyals. Understanding deep learning (still) requires rethinking generalization. *Communications of the ACM*, 64(3):107–115, 2021.
- Yifei Zhang, Hao Zhu, Zixing Song, Piotr Koniusz, and Irwin King. Spectral feature augmentation for graph contrastive learning and beyond. In *Proceedings of the AAAI Conference on Artificial Intelligence*, volume 37, pages 11289–11297, 2023.
- Zhilu Zhang and Mert Sabuncu. Generalized cross entropy loss for training deep neural networks with noisy labels. *Advances in neural information processing systems*, 31, 2018.
- Hao Zhu and Piotr Koniusz. Simple spectral graph convolution. In *International Conference on Learning Representations*, 2020.

Jun Zhuang and Mohammad Al Hasan. Defending graph convolutional networks against dynamic graph perturbations via bayesian self-supervision. In *Proceedings of the AAAI Conference on Artificial Intelligence*, volume 36, pages 4405–4413, 2022.

## A THEORETICAL RESULTS

First, recall that the optimization problem of the low-rank transductive classification is

$$\min_{\mathbf{W}} \frac{1}{m} \sum_{v_i \in \mathcal{V}_{\mathcal{L}}} \text{KL}(\mathbf{y}_i, [\text{softmax}(\mathbf{HW})]_i).$$

We then present the proof of Theorem 4.1.

**Proof of Theorem 4.1.** It can be verified that at the  $t$ -th iteration of gradient descent for  $t \geq 1$ , we have

$$\mathbf{W}^{(t)} = \mathbf{W}^{(t-1)} - \eta \mathbf{H}^\top (\mathbf{HW}^{(t-1)} - \mathbf{Y}). \quad (5)$$

It follows by (5) that

$$\mathbf{HW}^{(t)} = \mathbf{HW}^{(t-1)} - \eta \mathbf{K} (\mathbf{HW}^{(t-1)} - \mathbf{Y}), \quad (6)$$

where  $\mathbf{K} = \mathbf{HH}^\top$ . With  $\mathbf{F}(\mathbf{W}, t) = \mathbf{HW}^{(t)}$ , it follows by (6) that

$$\mathbf{F}(\mathbf{W}, t) - \mathbf{Y} = (\mathbf{I}_N - \eta \mathbf{K}) (\mathbf{F}(\mathbf{W}, t-1) - \mathbf{Y}).$$

It follows from the above equality that

$$\mathbf{F}(\mathbf{W}, t) - \mathbf{Y} = (\mathbf{I}_N - \eta \mathbf{K})^t (\mathbf{F}(\mathbf{W}, 0) - \mathbf{Y}) = -(\mathbf{I}_N - \eta \mathbf{K})^t \mathbf{Y},$$

so that

$$\|\mathbf{F}(\mathbf{W}, t) - \mathbf{Y}\|_{\mathbf{F}} \leq \|(\mathbf{I}_N - \eta \mathbf{K})^t \mathbf{Y}\|_{\mathbf{F}}. \quad (7)$$

As a result of (7), we have

$$\|[\mathbf{F}(\mathbf{W}, t) - \mathbf{Y}]_{\mathcal{L}}\|_{\mathbf{F}} \leq \|(\mathbf{I}_N - \eta \mathbf{K})^t \mathbf{Y}\|_{\mathbf{F}}. \quad (8)$$

We apply [Yang, 2023, Corollary 3.7] to obtain the following bound for the test loss  $\frac{1}{u} \|[\mathbf{F}(\mathbf{W}, t) - \mathbf{Y}]_{\mathcal{U}}\|_{\mathbf{F}}^2$ :

$$\frac{1}{u} \|[\mathbf{F}(\mathbf{W}, t) - \mathbf{Y}]_{\mathcal{U}}\|_{\mathbf{F}}^2 \leq \frac{c_0}{m} \|[\mathbf{F}(\mathbf{W}, t) - \mathbf{Y}]_{\mathcal{L}}\|_{\mathbf{F}}^2 + c_1 \min_{0 \leq Q \leq n} r(u, m, Q) + \frac{c_2 x}{u}, \quad (9)$$

with

$$r(u, m, Q) := Q \left( \frac{1}{u} + \frac{1}{m} \right) + \left( \sqrt{\frac{\sum_{q=Q+1}^n \hat{\lambda}_q}{u}} + \sqrt{\frac{\sum_{q=Q+1}^n \hat{\lambda}_q}{m}} \right).$$

where  $c_0, c_1, c_2$  are positive numbers depending on  $\mathbf{U}$ ,  $\{\hat{\lambda}_i\}_{i=1}^r$ , and  $\tau_0$  with  $\tau_0^2 = \max_{i \in [N]} \mathbf{K}_{ii}$ .

It follows by (7) and (9) with  $Q = r_0$  that

$$\begin{aligned} & \frac{1}{u} \|[\mathbf{F}(\mathbf{W}, t) - \mathbf{Y}]_{\mathcal{U}}\|_{\mathbf{F}}^2 \\ & \leq \frac{c_0}{m} \|[\mathbf{F}(\mathbf{W}, t) - \mathbf{Y}]_{\mathcal{L}}\|_{\mathbf{F}}^2 + c_1 r_0 \left( \frac{1}{u} + \frac{1}{m} \right) + \left( \sqrt{\frac{\sum_{q=r_0+1}^n \hat{\lambda}_q}{u}} + \sqrt{\frac{\sum_{q=r_0+1}^n \hat{\lambda}_q}{m}} \right) + \frac{c_2 x}{u}, \end{aligned} \quad (10)$$

which completes the proof.  $\square$



## B IMPLEMENTATION DETAILS

### B.1 COMPARED METHODS

To demonstrate the power of LR-GCL in learning robust node representation, we compare LR-GCL with two robust contrastive learning baselines, Jo-SRC and Sel-CL, which select clean samples for image data. Since their sample selection methods are general and not limited to the image domain, we adopt these two baselines in our experiments. Next, we introduce the implementation details of applying Jo-SRC and Sel-CL on graph data.

**Jo-SRC** [Yao et al., 2021]: Jo-SRC is a robust contrastive learning method proposed for image classification. It selects clean samples for training by adopting the Jensen-Shannon divergence to measure the likelihood of each sample being clean. Because this method is a general selection strategy on the representation space, it is adapted to selecting clean samples in the representation space of nodes in GCL. It also introduces a consistency regularization term to the contrastive loss to improve the robustness. To get a competitive robust GCL baseline, we apply the sample selection strategy and the consistency regularization proposed by Jo-SRC to state-of-the-art GCL methods MVGRL, MERIT, and SUGRL. We add the regularization term in Jo-SRC to the graph contrastive loss. The GCL encoders are trained only on the clean samples selected by Jo-SRC. We only report the best results for comparison, which are achieved by applying Jo-SRC to MERIT.

**Sel-CL** [Li et al., 2022]: Sel-CL is a supervised contrastive learning proposed to learn robust pre-trained representations for image classification. It proposes to select confident contrastive pairs in the contrastive learning frameworks. Sel-CL first selects confident examples by measuring the agreement between learned representations and labels generated by label propagation with cross-entropy loss. Next, Sel-CL selects contrastive pairs from those with selected confident examples in them. This method is also a general sample selection strategy on a learned representation space. So we can adapt Sel-CL to the node representation space to select confident pairs for GCL. In this process, they only select contrastive pairs whose representation similarity is higher than a dynamic threshold. In our experiments, we also adopt the confident contrastive pair selection strategy to the state-of-the-art GCL methods MVGRL, MERIT, and SUGRL. With the same GCL framework, GCL encoders are trained only on the confident pairs selected by Sel-CL. We only report the best results for comparison, which are achieved by applying Sel-CL to MERIT.

## C ADDITIONAL EXPERIMENTAL RESULTS

### C.1 NODE CLASSIFICATION ON WIKI-CS, AMAZON-COMPUTERS, AND AMAZON-PHOTOS

The results for node classification with symmetric label noise, asymmetric label noise, and attribute noise on Wiki-CS, Amazon-Computers, and Amazon-Photos are shown in Table 5. It is observed that LR-GCL also outperforms all the baselines for node classification with both label noise and attribute noise on these three benchmark datasets.

### C.2 NODE CLASSIFICATION RESULTS FOR GCL METHODS WITH DIFFERENT TYPES OF CLASSIFIERS

Existing GCL methods, such as MERIT, SUGRL, and SFA, first train a graph encoder with graph contrastive learning objectives such as InfoNCE [Jin et al., 2021]. After obtaining the node representation learned by contrastive learning, a linear layer for classification is trained in the supervised setting. In contrast, LR-GCL adopts a transductive classifier on top of the node representation obtained by contrastive learning. For fair comparisons with previous GCL methods, we also train the compared GCL baselines with the same transductive classifier as in LR-GCL and a two-layer transductive GCN classifier. The results with different types of classifiers are deferred in Section C.2 of the supplementary.

### C.3 TRAINING TIME COMPARISONS AND STUDY ON DIFFERENT RANKS

In this section, we first compare the training time of LR-GCL against other baseline methods on all benchmark datasets. For our method, we include the training time of robust graph contrastive learning, the time of the SVD computation of the kernel, and the training time of the transductive classifier. For graph contrastive learning methods, we include both the training time of the GCL encoder and the downstream classifier. We evaluate the training time on one 80 GB A100 GPU. The results are shown in Table 7. It is observed that the LR-GCL takes similar training time as baseline GCL methods such as SFA and MERIT.

Table 5: Performance comparison for node classification on Wiki-CS, Amazon-Computers, and Amazon-Photos with asymmetric label noise, symmetric label noise, and attribute noise.

Dataset	Methods	Noise Level									
		0	40			60			80		
		-	Asymmetric	Symmetric	Attribute	Asymmetric	Symmetric	Attribute	Asymmetric	Symmetric	Attribute
Wiki-CS	GCN	0.918±0.001	0.645±0.009	0.656±0.006	0.702±0.010	0.511±0.013	0.501±0.009	0.531±0.010	0.429±0.022	0.389±0.011	0.415±0.013
	S <sup>2</sup> GC	0.918±0.001	0.657±0.012	0.663±0.006	0.713±0.010	0.516±0.013	0.514±0.009	0.556±0.009	0.437±0.020	0.396±0.010	0.422±0.012
	GCE	0.922±0.003	0.662±0.017	0.659±0.007	0.705±0.014	0.515±0.016	0.502±0.007	0.539±0.009	0.443±0.017	0.389±0.012	0.412±0.011
	UnionNET	0.918±0.002	0.669±0.023	0.671±0.013	0.706±0.012	0.525±0.011	0.529±0.011	0.540±0.012	0.458±0.015	0.401±0.011	0.420±0.007
	NRGNN	0.919±0.002	0.678±0.014	0.689±0.009	0.705±0.012	0.545±0.021	0.556±0.011	0.546±0.011	0.461±0.012	0.410±0.012	0.417±0.007
	RTGNN	0.920±0.005	0.678±0.012	0.691±0.009	0.712±0.008	0.559±0.010	0.569±0.011	0.560±0.008	0.455±0.015	0.415±0.015	0.412±0.014
	SUGRL	0.922±0.005	0.675±0.010	0.695±0.010	0.714±0.006	0.550±0.011	0.560±0.011	0.561±0.007	0.449±0.011	0.411±0.011	0.429±0.008
	MERIT	0.924±0.004	0.679±0.011	0.689±0.008	0.709±0.005	0.552±0.014	0.562±0.014	0.562±0.011	0.452±0.013	0.403±0.013	0.426±0.005
	ARIEL	0.925±0.004	0.682±0.011	0.699±0.009	0.712±0.005	0.555±0.011	0.566±0.011	0.556±0.011	0.454±0.014	0.415±0.019	0.427±0.013
	SFA	0.925±0.009	0.682±0.011	0.690±0.012	0.715±0.012	0.555±0.015	0.567±0.014	0.565±0.013	0.458±0.013	0.402±0.013	0.429±0.015
	Sel-Cl	0.922±0.008	0.684±0.009	0.694±0.012	0.714±0.010	0.557±0.013	0.568±0.013	0.566±0.010	0.457±0.013	0.412±0.017	0.425±0.009
	Jo-SRC	0.921±0.005	0.684±0.011	0.695±0.004	0.709±0.007	0.560±0.011	0.566±0.011	0.561±0.009	0.456±0.013	0.410±0.018	0.428±0.010
	GRAND+	0.927±0.004	0.682±0.011	0.693±0.006	0.715±0.008	0.554±0.008	0.568±0.013	0.557±0.011	0.455±0.012	0.416±0.013	0.428±0.011
	LR-GCL	<b>0.933±0.006</b>	<b>0.699±0.015</b>	<b>0.721±0.011</b>	<b>0.742±0.015</b>	<b>0.575±0.014</b>	<b>0.595±0.018</b>	<b>0.588±0.015</b>	<b>0.469±0.015</b>	<b>0.416±0.015</b>	<b>0.453±0.017</b>
	Amazon-Computers	GCN	0.815±0.005	0.547±0.015	0.636±0.007	0.639±0.008	0.405±0.014	0.517±0.010	0.439±0.012	0.265±0.012	0.354±0.014
S <sup>2</sup> GC		0.835±0.002	0.569±0.007	0.664±0.007	0.661±0.007	0.422±0.010	0.535±0.010	0.454±0.011	0.279±0.014	0.366±0.014	0.320±0.013
GCE		0.819±0.004	0.573±0.011	0.652±0.008	0.650±0.014	0.449±0.011	0.509±0.011	0.445±0.015	0.280±0.013	0.353±0.013	0.325±0.015
UnionNET		0.820±0.006	0.569±0.014	0.664±0.007	0.653±0.012	0.452±0.010	0.541±0.010	0.450±0.009	0.283±0.014	0.370±0.011	0.320±0.012
NRGNN		0.822±0.006	0.571±0.019	0.676±0.007	0.645±0.012	0.470±0.014	0.548±0.014	0.451±0.011	0.282±0.022	0.373±0.012	0.326±0.010
RTGNN		0.828±0.003	0.570±0.010	0.682±0.008	0.678±0.011	0.474±0.011	0.555±0.010	0.457±0.009	0.280±0.011	0.386±0.014	0.342±0.016
SUGRL		0.834±0.005	0.564±0.011	0.674±0.012	0.675±0.009	0.468±0.011	0.552±0.011	0.452±0.012	0.280±0.012	0.381±0.012	0.338±0.014
MERIT		0.831±0.005	0.560±0.008	0.670±0.008	0.671±0.009	0.467±0.013	0.547±0.013	0.450±0.014	0.277±0.013	0.385±0.013	0.335±0.009
ARIEL		0.843±0.004	0.573±0.013	0.681±0.010	0.675±0.009	0.471±0.012	0.553±0.012	0.455±0.014	0.284±0.014	0.389±0.013	0.343±0.013
SFA		0.839±0.010	0.564±0.011	0.677±0.013	0.676±0.015	0.473±0.014	0.549±0.014	0.457±0.014	0.282±0.016	0.389±0.013	0.344±0.017
Sel-Cl		0.828±0.002	0.570±0.010	0.685±0.012	0.676±0.009	0.472±0.013	0.554±0.014	0.455±0.011	0.282±0.017	0.389±0.013	0.341±0.015
Jo-SRC		0.825±0.005	0.571±0.006	0.684±0.013	0.679±0.007	0.473±0.011	0.556±0.008	0.458±0.012	0.285±0.013	0.387±0.018	0.345±0.018
GRAND+		0.858±0.006	0.570±0.009	0.682±0.007	0.678±0.011	0.472±0.010	0.554±0.008	0.456±0.012	0.284±0.015	0.387±0.015	0.345±0.013
LR-GCL		<b>0.858±0.006</b>	<b>0.589±0.011</b>	<b>0.713±0.007</b>	<b>0.695±0.011</b>	<b>0.492±0.011</b>	<b>0.587±0.013</b>	<b>0.477±0.012</b>	<b>0.306±0.012</b>	<b>0.419±0.012</b>	<b>0.363±0.011</b>
Amazon-Photos		GCN	0.703±0.005	0.475±0.023	0.501±0.013	0.529±0.009	0.351±0.014	0.341±0.014	0.372±0.011	0.291±0.022	0.281±0.019
	S <sup>2</sup> GC	0.736±0.005	0.488±0.013	0.528±0.013	0.553±0.008	0.363±0.012	0.367±0.014	0.390±0.013	0.304±0.024	0.284±0.019	0.288±0.011
	GCE	0.705±0.004	0.490±0.016	0.512±0.014	0.540±0.014	0.362±0.015	0.352±0.010	0.381±0.009	0.309±0.012	0.285±0.014	0.285±0.011
	UnionNET	0.706±0.006	0.499±0.015	0.547±0.014	0.545±0.013	0.379±0.013	0.399±0.013	0.379±0.012	0.322±0.021	0.302±0.013	0.290±0.012
	NRGNN	0.710±0.006	0.498±0.015	0.546±0.015	0.538±0.011	0.382±0.016	0.412±0.016	0.377±0.012	0.336±0.021	0.309±0.018	0.284±0.009
	RTGNN	0.746±0.008	0.498±0.007	0.556±0.007	0.550±0.012	0.392±0.010	0.424±0.013	0.390±0.014	0.348±0.017	0.308±0.016	0.302±0.011
	SUGRL	0.730±0.005	0.493±0.011	0.541±0.011	0.544±0.010	0.376±0.009	0.421±0.009	0.388±0.009	0.339±0.010	0.305±0.010	0.300±0.009
	MERIT	0.740±0.007	0.496±0.012	0.536±0.012	0.542±0.010	0.383±0.011	0.425±0.011	0.387±0.008	0.344±0.014	0.301±0.014	0.295±0.009
	SFA	0.740±0.011	0.502±0.014	0.532±0.015	0.547±0.013	0.390±0.014	0.433±0.014	0.389±0.012	0.347±0.016	0.312±0.015	0.299±0.013
	ARIEL	0.727±0.007	0.500±0.008	0.550±0.013	0.548±0.008	0.391±0.009	0.427±0.012	0.389±0.014	0.349±0.014	0.307±0.013	0.299±0.013
	Sel-Cl	0.725±0.008	0.499±0.012	0.551±0.010	0.549±0.008	0.389±0.011	0.426±0.008	0.391±0.020	0.350±0.018	0.310±0.015	0.300±0.017
	Jo-SRC	0.730±0.005	0.500±0.013	0.555±0.011	0.551±0.011	0.394±0.013	0.425±0.013	0.393±0.013	0.351±0.013	0.305±0.018	0.303±0.013
	GRAND+	0.756±0.004	0.497±0.010	0.553±0.010	0.552±0.011	0.390±0.013	0.422±0.013	0.387±0.013	0.348±0.013	0.309±0.014	0.302±0.012
	LR-GCL	<b>0.757±0.010</b>	<b>0.520±0.013</b>	<b>0.581±0.013</b>	<b>0.570±0.007</b>	<b>0.410±0.014</b>	<b>0.455±0.014</b>	<b>0.406±0.012</b>	<b>0.369±0.012</b>	<b>0.335±0.014</b>	<b>0.318±0.010</b>

Table 6: Performance comparison for node classification by inductive linear classifier, transductive two-layer GCN classifier, and transductive classifier used in LR-GCL. The comparisons are performed on Cora with asymmetric label noise, symmetric label noise, and attribute noise.

Methods	Noise Level									
	0	40			60			80		
	-	Asymmetric	Symmetric	Attribute	Asymmetric	Symmetric	Attribute	Asymmetric	Symmetric	Attribute
SUGRL (original, inductive classifier)	0.834±0.005	0.564±0.011	0.674±0.012	0.675±0.009	0.468±0.011	0.552±0.011	0.452±0.012	0.280±0.012	0.381±0.012	0.338±0.014
SUGRL + transductive GCN	0.833±0.006	0.562±0.013	0.675±0.015	0.673±0.012	0.470±0.011	0.551±0.011	0.454±0.012	0.280±0.012	0.380±0.012	0.340±0.014
SUGRL + linear transductive classifier	0.836±0.007	0.568±0.013	0.677±0.010	0.674±0.011	0.472±0.011	0.555±0.011	0.457±0.012	0.284±0.012	0.383±0.012	0.341±0.014
MERIT (original, inductive classifier)	0.831±0.005	0.560±0.008	0.670±0.008	0.671±0.009	0.467±0.013	0.547±0.013	0.450±0.014	0.277±0.013	0.385±0.013	0.335±0.009
MERIT + transductive GCN	0.831±0.007	0.562±0.011	0.668±0.013	0.672±0.014	0.466±0.013	0.549±0.015	0.451±0.016	0.276±0.012	0.382±0.014	0.337±0.013
MERIT + linear transductive classifier	0.833±0.003	0.562±0.014	0.673±0.012	0.673±0.011	0.466±0.015	0.546±0.016	0.453±0.017	0.280±0.016	0.386±0.011	0.336±0.014
SFA (original, inductive classifier)	0.839±0.010	0.564±0.011	0.677±0.013	0.676±0.015	0.473±0.014	0.549±0.014	0.457±0.014	0.282±0.016	0.389±0.013	0.344±0.017
SFA + transductive GCN	0.837±0.013	0.565±0.011	0.673±0.017	0.673±0.018	0.474±0.016	0.551±0.015	0.453±0.018	0.277±0.016	0.389±0.015	0.343±0.019
SFA + linear transductive classifier	0.841±0.015	0.566±0.013	0.678±0.014	0.679±0.014	0.477±0.015	0.552±0.012	0.456±0.016	0.284±0.017	0.391±0.015	0.348±0.019
LR-GCL	<b>0.858±0.006</b>	<b>0.589±0.011</b>	<b>0.713±0.007</b>	<b>0.695±0.011</b>	<b>0.492±0.011</b>	<b>0.587±0.013</b>	<b>0.477±0.012</b>	<b>0.306±0.012</b>	<b>0.419±0.012</b>	<b>0.363±0.011</b>

We also perform ablation study on the value of rank  $r$  in the optimization problem (3) for our low-rank transductive classifier. It is observed from Table 2 that the performance of our low-rank classifier is consistently close to the best performance among all the choices of the rank when  $r$  is between  $0.1 \min\{N, d\}$  and  $0.2 \min\{N, d\}$ .

Table 7: Training time (seconds) comparisons for node classification.

Methods	Cora	Citeseer	PubMed	Coauthor-CS	Wiki-CS	Computer	Photo	ogbn-arxiv
GCN	11.5	13.7	38.6	43.2	22.3	30.2	19.0	215.1
S <sup>2</sup> GC	20.7	22.5	47.2	57.2	27.6	38.5	22.2	243.7
GCE	32.6	36.9	67.3	80.8	37.6	50.1	32.2	346.1
UnionNET	67.5	69.7	100.5	124.2	53.2	69.2	45.3	479.3
NRGNN	72.4	80.5	142.7	189.4	74.3	97.2	62.4	650.2
RTGNN	143.3	169.5	299.5	353.5	153.7	201.5	124.2	1322.2
SUGRL	100.3	122.1	207.4	227.1	107.7	142.8	87.7	946.8
MERIT	167.2	179.2	336.7	375.3	172.3	226.5	140.6	1495.1
ARIEL	156.9	164.3	284.3	332.6	145.1	190.4	118.3	1261.4
SFA	237.5	269.4	457.1	492.3	233.5	304.5	187.2	2013.1
Sel-CI	177.3	189.9	313.5	352.5	161.7	211.1	130.9	1401.1
Jo-SRC	148.2	157.1	281.0	306.1	144.5	188.0	118.5	1256.0
GRAND+	57.4	68.4	101.7	124.2	54.8	73.8	44.5	479.2
LR-GCL	159.9	174.5	350.7	380.9	180.3	235.7	145.5	1552.7

#### C.4 EIGEN-PROJECTION AND CONCENTRATION ENTROPY

Figure 3 illustrates the eigen-projection and energy concentration ratio for more datasets.

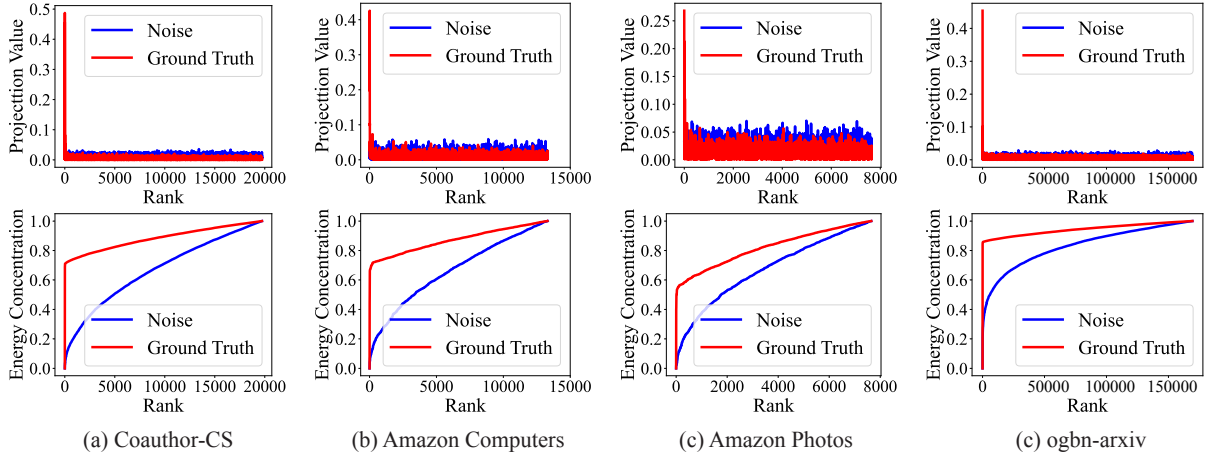


Figure 3: Eigen-projection (first row) and energy concentration (second row) on Coauthor-CS, Amazon-Computers, Amazon-Photos, and ogbn-arxiv. By the rank of  $0.2 \min\{N, d\}$ , the concentration entropy on Coauthor-CS, Amazon-Computers, Amazon-Photos, and ogbn-arxiv are 0.779, 0.809, 0.752, and 0.787.

#### C.5 VISUALIZATION OF CONFIDENCE SCORE

We visualize the confident nodes selected by BPL in the embedding space of the learned node representations in Figure 4. The node representations are visualized by the t-SNE figure. Each mark in t-SNE represents the representation of a node, and the color of the mark denotes the confidence of that node. The results are shown for different levels of attribute noise. It is observed from Figure 4 that confident nodes, which are redder in Figure 4, are well separated in the embedding space. With a higher level of attribute noise, the bluer nodes from different clusters blended around the cluster boundaries. In contrast, the redder nodes are still well separated and far away from cluster boundaries, which leads to more robustness and better performance in downstream tasks.

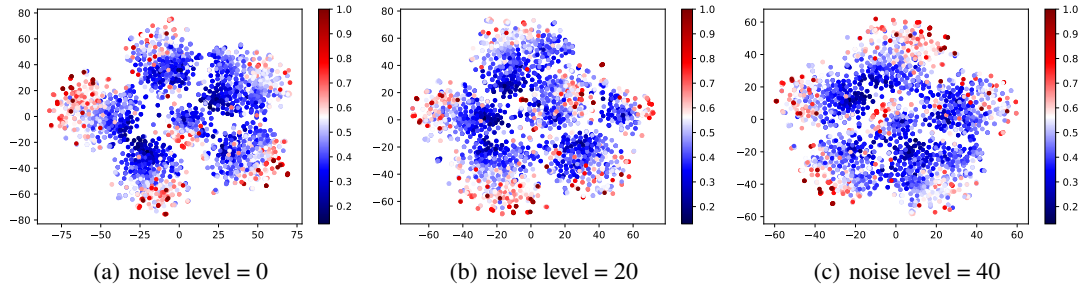


Figure 4: Visualization of confident nodes with different levels of attribute noise for semi-supervised node classification on Citeseer.

### C.6 STUDY IN THE KERNEL COMPLEXITY

With feature matrix  $\mathbf{H}$  produced by different encoders, we compute a kernel matrix  $\mathbf{K} = \widehat{\mathbf{A}}\mathbf{H}\mathbf{H}^\top\widehat{\mathbf{A}}^\top$  before and after optimization of problem (3). Score of  $\mathbf{K}$  is

$$\text{complexity of } \mathbf{K} = \min_{h \in [0, n]} \frac{h}{n} + \sqrt{\frac{\sum_{i=h+1}^n \widehat{\lambda}_i}{n}} \quad (11)$$

Also, compute  $\mathbf{K}$  for LR-GCL and other GCL baselines.

Datasets		MERIT	SFA	RGCL	LR-GCL
Cora	Complex.	0.5485	0.5749	0.5383	0.1675
	$h$	1455	1532	1431	433 (rank)
Citeseer	Complex.	0.4233	0.4546	0.4090	0.1178
	$h$	1347	1479	1330	366
PubMed	Complex.	0.9770	0.1095	0.0932	0.0674
	$h$	1690	1874	1667	1183
Wiki-CS	Complex.	0.1615	0.1762	0.1498	0.1062
	$h$	1784	1986	1639	1170
Amazon-Computers	Complex.	0.1132	0.1217	0.1110	0.0655
	$h$	1467	1579	1433	874
Amazon-Photos	Complex.	0.1875	0.2047	0.1823	0.1007
	$h$	1397	1532	1353	750
Coauthor-CS	Complex.	0.0764	0.0859	0.0749	0.0622
	$h$	1657	1874	1605	1120
ogbn-arxiv	Complex.	0.0124	0.0139	0.0117	0.0103
	$h$	1769	1920	1653	1354

Table 8: Comparisons in complexity of kernels.